

Measurement of the semileptonic charge asymmetry using $B_s^0 \rightarrow D_s \mu X$ decays

V.M. Abazov,³² B. Abbott,⁶⁹ B.S. Acharya,²⁶ M. Adams,⁴⁶ T. Adams,⁴⁴ G.D. Alexeev,³² G. Alkhalaf,³⁶ A. Alton,^{a, 58} G. Alverson,⁵⁷ A. Askew,⁴⁴ S. Atkins,⁵⁵ K. Augsten,⁷ C. Avila,⁵ F. Badaud,¹⁰ L. Bagby,⁴⁵ B. Baldin,⁴⁵ D.V. Bandurin,⁴⁴ S. Banerjee,²⁶ E. Barberis,⁵⁷ P. Baringer,⁵³ J.F. Bartlett,⁴⁵ U. Bassler,¹⁵ V. Bazterra,⁴⁶ A. Bean,⁵³ M. Begalli,² L. Bellantoni,⁴⁵ S.B. Beri,²⁴ G. Bernardi,¹⁴ R. Bernhard,¹⁹ I. Bertram,³⁹ M. Besançon,¹⁵ R. Beuselinck,⁴⁰ P.C. Bhat,⁴⁵ S. Bhatia,⁶⁰ V. Bhatnagar,²⁴ G. Blazey,⁴⁷ S. Blessing,⁴⁴ K. Bloom,⁶¹ A. Boehnlein,⁴⁵ D. Boline,⁶⁶ E.E. Boos,³⁴ G. Borissov,³⁹ T. Bose,⁵⁶ A. Brandt,⁷² O. Brandt,²⁰ R. Brock,⁵⁹ A. Bross,⁴⁵ D. Brown,¹⁴ J. Brown,¹⁴ X.B. Bu,⁴⁵ M. Buehler,⁴⁵ V. Buescher,²¹ V. Bunichev,³⁴ S. Burdin,^{b, 39} C.P. Buszello,³⁸ E. Camacho-Pérez,²⁹ B.C.K. Casey,⁴⁵ H. Castilla-Valdez,²⁹ S. Caughron,⁵⁹ S. Chakrabarti,⁶⁶ D. Chakraborty,⁴⁷ K.M. Chan,⁵¹ A. Chandra,⁷⁴ E. Chapon,¹⁵ G. Chen,⁵³ S. Chevalier-Théry,¹⁵ D.K. Cho,⁷¹ S.W. Cho,²⁸ S. Choi,²⁸ B. Choudhary,²⁵ S. Cihangir,⁴⁵ D. Claes,⁶¹ J. Clutter,⁵³ M. Cooke,⁴⁵ W.E. Cooper,⁴⁵ M. Corcoran,⁷⁴ F. Couderc,¹⁵ M.-C. Cousinou,¹² A. Croc,¹⁵ D. Cutts,⁷¹ A. Das,⁴² G. Davies,⁴⁰ S.J. de Jong,^{30, 31} E. De La Cruz-Burelo,²⁹ F. Déliot,¹⁵ R. Demina,⁶⁵ D. Denisov,⁴⁵ S.P. Denisov,³⁵ S. Desai,⁴⁵ C. Deterre,¹⁵ K. DeVaughan,⁶¹ H.T. Diehl,⁴⁵ M. Diesburg,⁴⁵ P.F. Ding,⁴¹ A. Dominguez,⁶¹ A. Dubey,²⁵ L.V. Dudko,³⁴ D. Duggan,⁶² A. Duperrin,¹² S. Dutt,²⁴ A. Dyshkant,⁴⁷ M. Eads,⁶¹ D. Edmunds,⁵⁹ J. Ellison,⁴³ V.D. Elvira,⁴⁵ Y. Enari,¹⁴ H. Evans,⁴⁹ A. Evdokimov,⁶⁷ V.N. Evdokimov,³⁵ G. Facini,⁵⁷ L. Feng,⁴⁷ T. Ferbel,⁶⁵ F. Fiedler,²¹ F. Filthaut,^{30, 31} W. Fisher,⁵⁹ H.E. Fisk,⁴⁵ M. Fortner,⁴⁷ H. Fox,³⁹ S. Fuess,⁴⁵ A. Garcia-Bellido,⁶⁵ J.A. García-González,²⁹ G.A. García-Guerra,^{c, 29} V. Gavrilov,³³ P. Gay,¹⁰ W. Geng,^{12, 59} D. Gerbaudo,⁶³ C.E. Gerber,⁴⁶ Y. Gershtein,⁶² G. Ginther,^{45, 65} G. Golovanov,³² A. Goussiou,⁷⁶ P.D. Grannis,⁶⁶ S. Greder,¹⁶ H. Greenlee,⁴⁵ G. Grenier,¹⁷ Ph. Gris,¹⁰ J.-F. Grivaz,¹³ A. Grohsjean,^{d, 15} S. Grünendahl,⁴⁵ M.W. Grünwald,²⁷ T. Guillemain,¹³ G. Gutierrez,⁴⁵ P. Gutierrez,⁶⁹ S. Hagopian,⁴⁴ J. Haley,⁵⁷ L. Han,⁴ K. Harder,⁴¹ A. Harel,⁶⁵ J.M. Hauptman,⁵² J. Hays,⁴⁰ T. Head,⁴¹ T. Hebbeker,¹⁸ D. Hedin,⁴⁷ H. Hegab,⁷⁰ A.P. Heinson,⁴³ U. Heintz,⁷¹ C. Hensel,²⁰ I. Heredia-De La Cruz,²⁹ K. Herner,⁵⁸ G. Hesketh,^{f, 41} M.D. Hildreth,⁵¹ R. Hirosky,⁷⁵ T. Hoang,⁴⁴ J.D. Hobbs,⁶⁶ B. Hoeneisen,⁹ J. Hogan,⁷⁴ M. Hohlfeld,²¹ I. Howley,⁷² Z. Hubacek,^{7, 15} V. Hynek,⁷ I. Iashvili,⁶⁴ Y. Ilchenko,⁷³ R. Illingworth,⁴⁵ A.S. Ito,⁴⁵ S. Jabeen,⁷¹ M. Jaffré,¹³ A. Jayasinghe,⁶⁹ M.S. Jeong,²⁸ R. Jesik,⁴⁰ K. Johns,⁴² E. Johnson,⁵⁹ M. Johnson,⁴⁵ A. Jonckheere,⁴⁵ P. Jonsson,⁴⁰ J. Joshi,⁴³ A.W. Jung,⁴⁵ A. Juste,³⁷ K. Kaadze,⁵⁴ E. Kajfasz,¹² D. Karmanov,³⁴ P.A. Kasper,⁴⁵ I. Katsanos,⁶¹ R. Kehoe,⁷³ S. Kermiche,¹² N. Khalatyan,⁴⁵ A. Khanov,⁷⁰ A. Kharchilava,⁶⁴ Y.N. Kharzheev,³² I. Kiselevich,³³ J.M. Kohli,²⁴ A.V. Kozelov,³⁵ J. Kraus,⁶⁰ S. Kulikov,³⁵ A. Kumar,⁶⁴ A. Kupco,⁸ T. Kurča,¹⁷ V.A. Kuzmin,³⁴ S. Lammers,⁴⁹ G. Landsberg,⁷¹ P. Lebrun,¹⁷ H.S. Lee,²⁸ S.W. Lee,⁵² W.M. Lee,⁴⁵ X. Lei,⁴² J. Lellouch,¹⁴ H. Li,¹¹ L. Li,⁴³ Q.Z. Li,⁴⁵ J.K. Lim,²⁸ D. Lincoln,⁴⁵ J. Linnemann,⁵⁹ V.V. Lipaev,³⁵ R. Lipton,⁴⁵ H. Liu,⁷³ Y. Liu,⁴ A. Lobodenko,³⁶ M. Lokajicek,⁸ R. Lopes de Sa,⁶⁶ H.J. Lubatti,⁷⁶ R. Luna-Garcia,^{g, 29} A.L. Lyon,⁴⁵ A.K.A. Maciel,¹ R. Madar,¹⁵ R. Magaña-Villalba,²⁹ S. Malik,⁶¹ V.L. Malyshev,³² Y. Maravin,⁵⁴ J. Martínez-Ortega,²⁹ R. McCarthy,⁶⁶ C.L. McGivern,⁴¹ M.M. Meijer,^{30, 31} A. Melnitchouk,⁶⁰ D. Menezes,⁴⁷ P.G. Mercadante,³ M. Merkin,³⁴ A. Meyer,¹⁸ J. Meyer,²⁰ F. Miconi,¹⁶ N.K. Mondal,²⁶ M. Mulhearn,⁷⁵ E. Nagy,¹² M. Naimuddin,²⁵ M. Narain,⁷¹ R. Nayyar,⁴² H.A. Neal,⁵⁸ J.P. Negret,⁵ P. Neustroev,³⁶ T. Nunnemann,²² J. Orduna,⁷⁴ N. Osman,¹² J. Osta,⁵¹ M. Padilla,⁴³ A. Pal,⁷² N. Parashar,⁵⁰ V. Parihar,⁷¹ S.K. Park,²⁸ R. Partridge,^{e, 71} N. Parua,⁴⁹ A. Patwa,⁶⁷ B. Penning,⁴⁵ M. Perfilov,³⁴ Y. Peters,⁴¹ K. Petridis,⁴¹ G. Petrillo,⁶⁵ P. Pétroff,¹³ M.-A. Pleier,⁶⁷ P.L.M. Podesta-Lerma,^{h, 29} V.M. Podstavkov,⁴⁵ A.V. Popov,³⁵ M. Prewitt,⁷⁴ D. Price,⁴⁹ N. Prokopenko,³⁵ J. Qian,⁵⁸ A. Quadt,²⁰ B. Quinn,⁶⁰ M.S. Rangel,¹ K. Ranjan,²⁵ P.N. Ratoff,³⁹ I. Razumov,³⁵ P. Renkel,⁷³ I. Ripp-Baudot,¹⁶ F. Rizatdinova,⁷⁰ M. Rominsky,⁴⁵ A. Ross,³⁹ C. Royon,¹⁵ P. Rubinov,⁴⁵ R. Ruchti,⁵¹ G. Sajot,¹¹ P. Salcido,⁴⁷ A. Sánchez-Hernández,²⁹ M.P. Sanders,²² A.S. Santos,^{i, 1} G. Savage,⁴⁵ L. Sawyer,⁵⁵ T. Scanlon,⁴⁰ R.D. Schamberger,⁶⁶ Y. Scheglov,³⁶ H. Schellman,⁴⁸ S. Schlobohm,⁷⁶ C. Schwanenberger,⁴¹ R. Schwienhorst,⁵⁹ J. Sekaric,⁵³ H. Severini,⁶⁹ E. Shabalina,²⁰ V. Shary,¹⁵ S. Shaw,⁵⁹ A.A. Shchukin,³⁵ R.K. Shivpuri,²⁵ V. Simak,⁷ P. Skubic,⁶⁹ P. Slattery,⁶⁵ D. Smirnov,⁵¹ K.J. Smith,⁶⁴ G.R. Snow,⁶¹ J. Snow,⁶⁸ S. Snyder,⁶⁷ S. Söldner-Rembold,⁴¹ L. Sonnenschein,¹⁸ K. Soustruznik,⁶ J. Stark,¹¹ D.A. Stoyanova,³⁵ M. Strauss,⁶⁹ L. Suter,⁴¹ P. Svoisky,⁶⁹ M. Takahashi,⁴¹ M. Titov,¹⁵ V.V. Tokmenin,³² Y.-T. Tsai,⁶⁵ K. Tschann-Grimm,⁶⁶ D. Tsybychev,⁶⁶ B. Tuchming,¹⁵ C. Tully,⁶³ L. Uvarov,³⁶ S. Uvarov,³⁶ S. Uzunyan,⁴⁷ R. Van Kooten,⁴⁹ W.M. van Leeuwen,³⁰ N. Varelas,⁴⁶ E.W. Varnes,⁴² I.A. Vasilyev,³⁵ P. Verdier,¹⁷

A.Y. Verkheev,³² L.S. Vertogradov,³² M. Verzocchi,⁴⁵ M. Vesterinen,⁴¹ D. Vilanova,¹⁵ P. Vokac,⁷ H.D. Wahl,⁴⁴ M.H.L.S. Wang,⁴⁵ J. Warchol,⁵¹ G. Watts,⁷⁶ M. Wayne,⁵¹ J. Weichert,²¹ L. Welty-Rieger,⁴⁸ A. White,⁷² D. Wicke,²³ M.R.J. Williams,³⁹ G.W. Wilson,⁵³ M. Wobisch,⁵⁵ D.R. Wood,⁵⁷ T.R. Wyatt,⁴¹ Y. Xie,⁴⁵ R. Yamada,⁴⁵ S. Yang,⁴ W.-C. Yang,⁴¹ T. Yasuda,⁴⁵ Y.A. Yatsunenkov,³² W. Ye,⁶⁶ Z. Ye,⁴⁵ H. Yin,⁴⁵ K. Yip,⁶⁷ S.W. Youn,⁴⁵ J.M. Yu,⁵⁸ J. Zennamo,⁶⁴ T. Zhao,⁷⁶ T.G. Zhao,⁴¹ B. Zhou,⁵⁸ J. Zhu,⁵⁸ M. Zielinski,⁶⁵ D. Zieminska,⁴⁹ and L. Zivkovic⁷¹

(The D0 Collaboration*)

¹LAFEX, Centro Brasileiro de Pesquisas Físicas, Rio de Janeiro, Brazil

²Universidade do Estado do Rio de Janeiro, Rio de Janeiro, Brazil

³Universidade Federal do ABC, Santo André, Brazil

⁴University of Science and Technology of China, Hefei, People's Republic of China

⁵Universidad de los Andes, Bogotá, Colombia

⁶Charles University, Faculty of Mathematics and Physics,
Center for Particle Physics, Prague, Czech Republic

⁷Czech Technical University in Prague, Prague, Czech Republic

⁸Center for Particle Physics, Institute of Physics,
Academy of Sciences of the Czech Republic, Prague, Czech Republic

⁹Universidad San Francisco de Quito, Quito, Ecuador

¹⁰LPC, Université Blaise Pascal, CNRS/IN2P3, Clermont, France

¹¹LPSC, Université Joseph Fourier Grenoble 1, CNRS/IN2P3,
Institut National Polytechnique de Grenoble, Grenoble, France

¹²CPPM, Aix-Marseille Université, CNRS/IN2P3, Marseille, France

¹³LAL, Université Paris-Sud, CNRS/IN2P3, Orsay, France

¹⁴LPNHE, Universités Paris VI and VII, CNRS/IN2P3, Paris, France

¹⁵CEA, Irfu, SPP, Saclay, France

¹⁶IPHC, Université de Strasbourg, CNRS/IN2P3, Strasbourg, France

¹⁷IPNL, Université Lyon 1, CNRS/IN2P3, Villeurbanne, France and Université de Lyon, Lyon, France

¹⁸III. Physikalisches Institut A, RWTH Aachen University, Aachen, Germany

¹⁹Physikalisches Institut, Universität Freiburg, Freiburg, Germany

²⁰II. Physikalisches Institut, Georg-August-Universität Göttingen, Göttingen, Germany

²¹Institut für Physik, Universität Mainz, Mainz, Germany

²²Ludwig-Maximilians-Universität München, München, Germany

²³Fachbereich Physik, Bergische Universität Wuppertal, Wuppertal, Germany

²⁴Panjab University, Chandigarh, India

²⁵Delhi University, Delhi, India

²⁶Tata Institute of Fundamental Research, Mumbai, India

²⁷University College Dublin, Dublin, Ireland

²⁸Korea Detector Laboratory, Korea University, Seoul, Korea

²⁹CINVESTAV, Mexico City, Mexico

³⁰Nikhef, Science Park, Amsterdam, the Netherlands

³¹Radboud University Nijmegen, Nijmegen, the Netherlands

³²Joint Institute for Nuclear Research, Dubna, Russia

³³Institute for Theoretical and Experimental Physics, Moscow, Russia

³⁴Moscow State University, Moscow, Russia

³⁵Institute for High Energy Physics, Protvino, Russia

³⁶Petersburg Nuclear Physics Institute, St. Petersburg, Russia

³⁷Institució Catalana de Recerca i Estudis Avançats (ICREA) and Institut de Física d'Altes Energies (IFAE), Barcelona, Spain

³⁸Uppsala University, Uppsala, Sweden

³⁹Lancaster University, Lancaster LA1 4YB, United Kingdom

⁴⁰Imperial College London, London SW7 2AZ, United Kingdom

⁴¹The University of Manchester, Manchester M13 9PL, United Kingdom

⁴²University of Arizona, Tucson, Arizona 85721, USA

⁴³University of California Riverside, Riverside, California 92521, USA

⁴⁴Florida State University, Tallahassee, Florida 32306, USA

⁴⁵Fermi National Accelerator Laboratory, Batavia, Illinois 60510, USA

⁴⁶University of Illinois at Chicago, Chicago, Illinois 60607, USA

⁴⁷Northern Illinois University, DeKalb, Illinois 60115, USA

⁴⁸Northwestern University, Evanston, Illinois 60208, USA

⁴⁹Indiana University, Bloomington, Indiana 47405, USA

⁵⁰Purdue University Calumet, Hammond, Indiana 46323, USA

⁵¹University of Notre Dame, Notre Dame, Indiana 46556, USA

⁵²Iowa State University, Ames, Iowa 50011, USA

⁵³University of Kansas, Lawrence, Kansas 66045, USA

- ⁵⁴Kansas State University, Manhattan, Kansas 66506, USA
⁵⁵Louisiana Tech University, Ruston, Louisiana 71272, USA
⁵⁶Boston University, Boston, Massachusetts 02215, USA
⁵⁷Northeastern University, Boston, Massachusetts 02115, USA
⁵⁸University of Michigan, Ann Arbor, Michigan 48109, USA
⁵⁹Michigan State University, East Lansing, Michigan 48824, USA
⁶⁰University of Mississippi, University, Mississippi 38677, USA
⁶¹University of Nebraska, Lincoln, Nebraska 68588, USA
⁶²Rutgers University, Piscataway, New Jersey 08855, USA
⁶³Princeton University, Princeton, New Jersey 08544, USA
⁶⁴State University of New York, Buffalo, New York 14260, USA
⁶⁵University of Rochester, Rochester, New York 14627, USA
⁶⁶State University of New York, Stony Brook, New York 11794, USA
⁶⁷Brookhaven National Laboratory, Upton, New York 11973, USA
⁶⁸Langston University, Langston, Oklahoma 73050, USA
⁶⁹University of Oklahoma, Norman, Oklahoma 73019, USA
⁷⁰Oklahoma State University, Stillwater, Oklahoma 74078, USA
⁷¹Brown University, Providence, Rhode Island 02912, USA
⁷²University of Texas, Arlington, Texas 76019, USA
⁷³Southern Methodist University, Dallas, Texas 75275, USA
⁷⁴Rice University, Houston, Texas 77005, USA
⁷⁵University of Virginia, Charlottesville, Virginia 22901, USA
⁷⁶University of Washington, Seattle, Washington 98195, USA
- (Dated: July 6, 2012)

We present a measurement of the time-integrated flavor-specific semileptonic charge asymmetry in the decays of B_s^0 mesons that have undergone flavor mixing, a_{sl}^s , using $B_s^0(\bar{B}_s^0) \rightarrow D_s^\mp \mu^\pm X$ decays, with $D_s^\mp \rightarrow \phi \pi^\mp$ and $\phi \rightarrow K^+ K^-$, using 10.4 fb^{-1} of proton-antiproton collisions collected by the D0 detector during Run II at the Fermilab Tevatron Collider. A fit to the difference between the time-integrated D_s^- and D_s^+ mass distributions of the B_s^0 and \bar{B}_s^0 candidates yields the flavor-specific asymmetry $a_{sl}^s = [-1.08 \pm 0.72 \text{ (stat)} \pm 0.17 \text{ (syst)}] \%$ which is the most precise measurement and in agreement with the standard model prediction.

PACS numbers: 11.30.Er, 13.20.He, 14.40.Nd

CP violation has been observed in the decay and mixing of neutral mesons containing strange, charm and bottom quarks. Currently all measurements of CP violation, either in decay, mixing or in the interference between the two, have been consistent with the presence of a single phase in the CKM matrix. An observation of anomalously large CP violation in B_s^0 oscillations can indicate the existence of physics beyond the standard model (SM) [1]. Measurements of the like-sign dimuon asymmetry by the D0 Collaboration [2, 3] show evidence of anomalously large CP-violating effects using data corresponding to 9 fb^{-1} of integrated luminosity. Assuming that this asymmetry originates from mixed neutral B mesons, the measured value is $A_{sl}^b = C_d a_{sl}^d + C_s a_{sl}^s = [-0.787 \pm 0.172 \text{ (stat.)} \pm 0.021 \text{ (syst.)}] \%$, where $a_{sl}^{s(d)}$ is the time-integrated flavor-specific semilep-

tonic charge asymmetry in $B_s^0(B_d^0)$ decays that have undergone flavor mixing and $C_{d(s)}$ is the fraction of $B_d^0(B_s^0)$ events. The value of a_{sl}^s is extracted from this measurement and found to be $a_{sl}^s = (-1.81 \pm 1.06) \%$ [3]. This Letter presents an independent measurement of a_{sl}^s using the decay $B_s^0 \rightarrow D_s^- \mu^+ X$, where $D_s^- \rightarrow \phi \pi^-$ and $\phi \rightarrow K^+ K^-$ (charge conjugate states are assumed in this Letter).

The asymmetry a_{sl}^s is defined as

$$a_{sl}^s = \frac{\Gamma(\bar{B}_s^0 \rightarrow B_s^0 \rightarrow \ell^+ \nu X) - \Gamma(B_s^0 \rightarrow \bar{B}_s^0 \rightarrow \ell^- \bar{\nu} \bar{X})}{\Gamma(\bar{B}_s^0 \rightarrow B_s^0 \rightarrow \ell^+ \nu X) + \Gamma(B_s^0 \rightarrow \bar{B}_s^0 \rightarrow \ell^- \bar{\nu} \bar{X})}, \quad (1)$$

where in this analysis $\ell = \mu$ and $X = D_s^{(*)-}$. This includes all decay processes of B_s^0 mesons that result in a D_s^- meson and an oppositely charged muon in the final state. To study CP violation, we identify events with the decay $B_s^0 \rightarrow D_s^- \mu^+ X$. The flavor of the B_s^0 meson at the time of decay is identified using the charge of the associated muon, and this analysis does not make use of initial-state tagging. The fraction of mixed events integrated over time is extracted using Monte Carlo (MC) simulations. We assume there is no production asymmetry between B_s^0 and \bar{B}_s^0 mesons, that there is no direct CP violation in the decay of D_s mesons to the indi-

*with visitors from ^aAugustana College, Sioux Falls, SD, USA, ^bThe University of Liverpool, Liverpool, UK, ^cUPIITA-IPN, Mexico City, Mexico, ^dDESY, Hamburg, Germany, ^eSLAC, Menlo Park, CA, USA, ^fUniversity College London, London, UK, ^gCentro de Investigacion en Computacion - IPN, Mexico City, Mexico, ^hECFM, Universidad Autonoma de Sinaloa, Culiacán, Mexico and ⁱUniversidade Estadual Paulista, São Paulo, Brazil.

cated states or in the semileptonic decay of B_s^0 mesons, and that any CP violation in B_s^0 mesons only occurs in mixing. This analysis does not make use of the decay $D_s^- \rightarrow K^{*0}K^-$ as used in Ref. [4] as the expected statistical uncertainty in this channel is 2.5 times worse than the decay $D_s^- \rightarrow \phi\pi^-$.

The value of the SM prediction for $a_{\text{sl}}^s = (1.9 \pm 0.3) \times 10^{-5}$ [1] is negligible compared with current experimental precision. The best direct measurement of a_{sl}^s was performed by the D0 Collaboration using data corresponding to 5 fb^{-1} of integrated luminosity, giving $a_{\text{sl}}^s = [-0.17 \pm 0.91 \text{ (stat.)}_{-0.23}^{+0.12} \text{ (syst.)}] \%$ [4]. This Letter presents a new and improved measurement of a_{sl}^s using the full Tevatron data sample with an integrated luminosity of 10.4 fb^{-1} .

The measurement is performed using the raw asymmetry

$$A = \frac{N_{\mu^+D_s^-} - N_{\mu^-D_s^+}}{N_{\mu^+D_s^-} + N_{\mu^-D_s^+}}, \quad (2)$$

where $N_{\mu^+D_s^-}$ ($N_{\mu^-D_s^+}$) is the number of reconstructed $B_s^0 \rightarrow \mu^+D_s^-X$ ($B_s^0 \rightarrow \mu^-D_s^+X$) decays. The time-integrated flavor-specific semileptonic charge asymmetry in B_s^0 decays which have undergone flavor mixing, a_{sl}^s , is then given by

$$a_{\text{sl}}^s = \frac{A - A_\mu - A_{\text{track}}}{F_{B_s^0}^{\text{osc}}}, \quad (3)$$

where A_μ is the reconstruction asymmetry between positive and negatively charged muons in the detector [5], A_{track} is the asymmetry between positive and negative tracks, and $F_{B_s^0}^{\text{osc}}$ is the fraction of $D_s^- \rightarrow \phi\pi^-$ decays that originate from the decay of a B_s^0 meson after a $\bar{B}_s^0 \rightarrow B_s^0$ oscillation. The $F_{B_s^0}^{\text{osc}}$ factor corrects the measured asymmetry for the fraction of events in which the B_s^0 meson is mixed. While the data selection, fitting models, A_μ and A_{track} studies were studied, the value of the raw asymmetry was offset by an unknown arbitrary value and any distribution that gives an indication of the value of A was not examined.

The D0 detector has a central tracking system, consisting of a silicon microstrip tracker (SMT) and a central fiber tracker (CFT), both located within a 2 T superconducting solenoidal magnet [5, 6]. An outer muon system, at $|\eta| < 2$ [7], consists of a layer of tracking detectors and scintillation trigger counters in front of 1.8 T toroidal magnets, followed by two similar layers after the toroids [8].

The data are collected with a suite of single and dimuon triggers. The selection and reconstruction of $\mu^+D_s^-X$ decays requires tracks with at least two hits in both the CFT and SMT. Muons are required to have hits in at least two layers of the muon system, with segments reconstructed both inside and outside the toroid.

The muon track segment has to be matched to a particle found in the central tracking system which has momentum $p > 3 \text{ GeV}/c$ and transverse momentum $2 < p_T < 25 \text{ GeV}/c$.

The $D_s^- \rightarrow \phi\pi^-$; $\phi \rightarrow K^+K^-$ decay is reconstructed as follows. The two particles from the ϕ decay are assumed to be kaons and are required to have $p_T > 0.7 \text{ GeV}/c$, opposite charge and a mass $M(K^+K^-) < 1.07 \text{ GeV}/c^2$. The charge of the third particle, assumed to be the charged pion, has to be opposite to that of the muon with $0.5 < p_T < 25 \text{ GeV}/c$. The three tracks are combined to create a common D_s^- decay vertex using the algorithm described in Ref. [9]. To reduce combinatorial background, the D_s^- vertex is required to have a displacement from the $p\bar{p}$ interaction vertex (PV) in the transverse plane with a significance of at least four standard deviations. The cosine of the angle between the D_s^- momentum and the vector from the PV to the D_s^- decay vertex is required to be greater than 0.9. The trajectories of the muon and D_s^- candidates are required to be consistent with originating from a common vertex (assumed to be the B_s^0 decay vertex) and to have an effective mass of $2.6 < M(\mu^+D_s^-) < 5.4 \text{ GeV}/c^2$, consistent with coming from a B_s^0 semileptonic decay. The cosine of the angle between the combined $\mu^+D_s^-$ direction, an approximation of the B_s^0 direction in the direction from the PV to the B_s^0 decay vertex has to be greater than 0.95. The B_s^0 decay vertex has to be displaced from the PV in the transverse plane with a significance of at least four standard deviations. These angular criteria ensure that the D_s^- and μ^+ momenta are correlated with that of their B_s^0 parent and that the D_s^- is not mistakenly associated with a random muon. If more than one B_s^0 candidate passes the selection criteria in an event, then all candidates are included in the final sample.

To improve the significance of the B_s^0 selection we use a likelihood ratio taken from Refs. [10, 11]. It combines several discriminating variables: the helicity angle between the D_s^- and K^+ momenta in the center-of-mass frame of the ϕ meson; the isolation of the $\mu^+D_s^-$ system, defined as $I = p(\mu^+D_s^-)/[p(\mu^+D_s^-) + \Sigma p_i]$, where $p(\mu^+D_s^-)$ is the sum of the momenta of the three tracks that make up the D_s^- meson and Σp_i is the sum of momenta for all tracks not associated with the $\mu^+D_s^-$ in a cone of $\sqrt{(\Delta\phi)^2 + (\Delta\eta)^2} < 0.5$ around the $\mu^+D_s^-$ direction [7]; the χ^2 of the D_s^- vertex fit; the invariant masses $M(\mu^+D_s^-)$, $M(K^+K^-)$; and $p_T(K^+K^-)$.

The final requirement on the likelihood ratio variable, y_{sel} , is chosen to maximize the predicted ratio $N_S/\sqrt{N_S + N_B}$ in a data subsample corresponding to 20% of the full data sample, where N_S is the number of signal events and N_B is the number of background events determined from signal and sideband regions of the $M(K^+K^-\pi^-)$ distributions.

The $M(K^+K^-\pi^-)$ distribution is analysed in bins of $6 \text{ MeV}/c^2$, over a mass range of $1.7 < M(K^+K^-\pi^-) <$

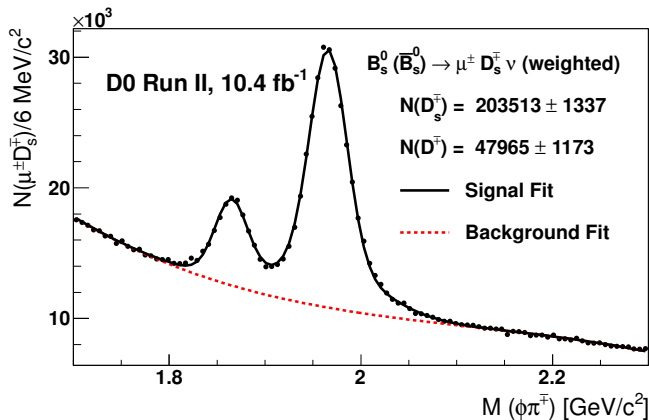


FIG. 1: The weighted $K^+K^-\pi^-$ invariant mass distribution for the $\mu^+\phi\pi^-$ sample with the solid line representing the signal fit and the dashed line showing the background fit. The lower mass peak is due to the decay $D^- \rightarrow \phi\pi^-$ and the second peak is due to the D_s^- meson decay.

$2.3 \text{ GeV}/c^2$. The number of events is extracted by fitting the data to a model using a χ^2 fit. The D_s^- meson mass distribution is well modelled in the D0 detector by two Gaussian functions constrained to have the same mean, but with different widths and relative normalizations. A second peak in the $M(K^+K^-\pi^-)$ distribution corresponding to the Cabibbo-suppressed decay of the D^- meson is also modelled by two Gaussian functions, and the combinatoric background by a third-order polynomial function. The number of D_s^- signal decays determined from the fit is $N(\mu^+D_s^-) = 215,763 \pm 1,467$, where the uncertainty is statistical.

The polarities of the toroidal and solenoidal magnetic fields are reversed on average every two weeks so that the four solenoid-toroid polarity combinations are exposed to approximately the same integrated luminosity. This allows for a cancellation of first-order effects related to instrumental asymmetries. To ensure full cancellation, the events are weighted according to the number of $\mu^+D_s^-$ decays for each data sample corresponding to a different configuration of the magnets' polarities. The data are then fitted to obtain the number of weighted events, $N(\mu^+D_s^-) = 203,513 \pm 1,337$. This is shown in Fig. 1, where the weighted $M(K^+K^-\pi^-)$ invariant mass distributions in data is compared to the signal and background fit.

The raw asymmetry (Eq. 2) is extracted by fitting the $M(\phi\pi^-)$ distribution of the D_s^- candidates using a χ^2 minimization. The fit is performed simultaneously on the sum and the difference of the $M(\phi\pi^-)$ and $M(\phi\pi^+)$ distributions for candidates with positively and negatively charged muons, respectively. The functions W used to model the two distributions are

$$W_{\text{sum}} = W^{\text{sig}}(D_s) + W^{\text{sig}}(D) + W_{\text{sum}}^{\text{bg}}, \quad (4)$$

$$W_{\text{diff}} = AW^{\text{sig}}(D_s) + A_D W^{\text{sig}}(D) + A_{\text{bg}} W_{\text{sum}}^{\text{bg}}, \quad (5)$$

where $W^{\text{sig}}(D_s)$, $W^{\text{sig}}(D)$ and $W_{\text{sum}}^{\text{bg}}$ describe the D_s^- , D^- mass peaks, and the combinatorial background, respectively. The asymmetry of the D^- mass peak is A_D , and A_{bg} is the asymmetry of the combinatorial background. The result of the fit is shown in Fig. 2 with fitted asymmetry parameters $A = (-0.40 \pm 0.33)\%$, $A_D = (-1.21 \pm 1.00)\%$, and $A_{\text{bg}} = (0.00 \pm 0.11)\%$.

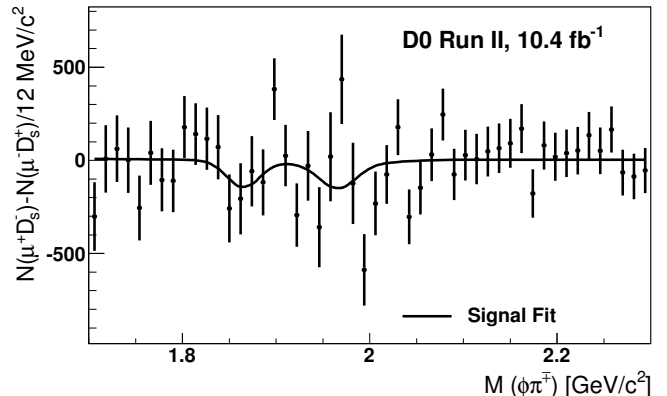


FIG. 2: The fit to the difference distribution for the data (for clarity the data has been rebinned).

The χ^2 of the fit model with respect to the difference histogram is 129.7/97 degrees of freedom over the whole mass range and 34.7 for 25 bins in the mass range $1.90 < M(\mu^+D_s^-) < 2.05 \text{ GeV}/c^2$, which corresponds to a p -value of 9.7%. The value of the extracted raw asymmetry, A , is checked by calculating the difference between the number of $\mu^+D_s^-$ and $\mu^-D_s^+$ events in the mass range $1.92 < M(\mu^+D_s^-) < 2.00 \text{ GeV}/c^2$ without using a fit. In this region we observe an asymmetry of $(-0.5 \pm 0.3)\%$ which is consistent with the value of A extracted by the fitting procedure.

To test the sensitivity of the fitting procedure, the charge of the muon is randomised to introduce an asymmetry signal. We use a range of raw signals from -2.0% to $+2.0\%$ in 0.2% steps with 1000 trials performed for each step, and the result of these pseudo-experiments, each with the same statistics as the measurement, is found. In each case, the central value of the asymmetry distribution is consistent with the input value with a fitted width of 0.33% and no observable bias. The uncertainty found in data agrees with this expected statistical sensitivity.

Systematic uncertainties in the fitting method are evaluated by making reasonable variations to the fitting procedure. The mass range of the fit is shifted from $1.700 < M(K^+K^-\pi^-) < 2.300 \text{ GeV}/c^2$ to $1.724 < M(K^+K^-\pi^-) < 2.270 \text{ GeV}/c^2$. The functions modelling the signal, W^{sig} , are modified so that the D^- and D_s^- peaks are fitted by single Gaussian functions. The background function, $W_{\text{sum}}^{\text{bg}}$, is varied from a second-order polynomial function to a fifth-order polynomial function,

and the asymmetry is extracted. Instead of setting the background of W_{diff} to $A_{\text{bg}}W_{\text{sum}}^{\text{bg}}$, the background is either set to zero, a constant, or a polynomial function of up to degree three. The width of the mass bins is varied between 2 and 12 MeV/ c^2 . Instead of using the fitted number of B_s^0 decays per magnet polarity to weight the events, the total number of candidates in the mass range $1.7 < M(K^+K^-\pi^-) < 2.3$ GeV/ c^2 is used. The systematic uncertainty is assigned to be half of the maximal variation in the asymmetry for each of these sources, added in quadrature. The total effect of all of these systematic sources of uncertainty is a systematic uncertainty of 0.051% on the raw asymmetry A , giving

$$A = [-0.40 \pm 0.33 (\text{stat.}) \pm 0.05 (\text{syst.})] \% \quad (6)$$

To extract a_{sl}^s from the raw asymmetry, corrections to the charge asymmetries in the reconstruction have to be made. In this decay channel any asymmetry between the reconstruction of K^+ and K^- mesons cancels as we require that the two kaons form a ϕ meson. The remaining asymmetries are the track reconstruction asymmetry A_{track} and the muon reconstruction asymmetry A_μ .

The residual detector tracking asymmetry, A_{track} , has been studied in Ref. [2] and by using $K_S^0 \rightarrow \pi^+\pi^-$ and $K^{*\pm} \rightarrow K_S^0\pi^\pm$ decays. No significant residual track reconstruction asymmetries are found and no correction for tracking asymmetries need to be applied. The tracking asymmetry of charged pions has been studied using MC simulations of the detector. The asymmetry is found to be less than 0.05%, which is assigned as a systematic uncertainty. The muon and the pion have opposite charge, so any remaining track asymmetries will cancel to first order.

The residual reconstruction asymmetry of the muon system, A_μ , has been measured using $J/\psi \rightarrow \mu^+\mu^-$ decays as described in [2, 3]. This asymmetry is determined as a function of p_T and $|\eta|$ of the muons, and the correction is obtained by a weighted average over the normalized yields, as determined from fits to the $M(\phi\pi^-)$ distribution. The resulting correction is $A_\mu = [0.11 \pm 0.06 (\text{syst.})] \%$, which also includes the systematic uncertainty due to track reconstruction.

The remaining variable required is $F_{B_s^0}^{\text{osc}}$ (Eq. 3), which is the only correction extracted from a MC simulation. The D_s^- signal decays can also be produced via the decay of B_d^0 mesons, B^\pm mesons, and from prompt $c\bar{c}$ production. The B_s^0 (B_d^0) mesons can oscillate to \bar{B}_s^0 (\bar{B}_d^0) states before decaying. We split these MC samples into mixed and unmixed decays. This classification is inclusive and includes most intermediate excited states of both B and D meson decays.

The MC sample is created using the PYTHIA event generator [12] modified to use EVTGEN [13] for the decay of hadrons containing b and c quarks. Events recorded in random beam crossings are overlaid over the simulated

events to quantify the effect of additional collisions in the same or nearby bunch crossings. The PYTHIA inclusive jet production model is used and events are selected that contain at least one muon and a $D_s^- \rightarrow \phi\pi^-$; $\phi \rightarrow K^+K^-$ decay. The generated events are processed by the full simulation chain, and then by the same reconstruction and selection algorithms as used to select events from data. Each event is classified based on the decay chain that is matched to the reconstructed particles.

The mean proper decay lengths of the b hadrons are fixed in the simulation to values close to the current world-average values [14]. To correct for these differences, a correction is applied to all non-prompt events in simulation, based on the generated lifetime of the B candidate, to give the appropriate world-average B meson lifetimes and measured value of the width difference $\Delta\Gamma_s$ [15].

To estimate the effects of trigger selection and track reconstruction, we weight each event as a function of p_T of the reconstructed muon so that it matches the distribution in the data, and as a function of the lifetime to ensure that the B -meson lifetimes and $\Delta\Gamma_s$ match the world-average [14].

In the case of the B_s^0 meson, the time-integrated oscillation probability is essentially 50% and is insensitive to the exact value of ΔM_s . Combining the fraction of B_s^0 decays in the sample and the time-integrated oscillation probability, we find $F_{B_s^0}^{\text{osc}} = 0.465$.

To determine the systematic uncertainty on $F_{B_s^0}^{\text{osc}}$, the branching ratios and production fractions of B mesons are varied by their uncertainties. We also vary the B -meson lifetimes and $\Delta\Gamma_s$ and use a coarser p_T binning in the p_T event weighting. The total resulting systematic uncertainty on $F_{B_s^0}^{\text{osc}}$ is determined to be 0.017 that includes the statistical uncertainty from the MC simulation. An asymmetry of B_d^0 decays of 1% would contribute 0.005% to the total asymmetry, which is negligible compared to the statistical uncertainties and therefore neglected.

The uncertainty due to the fitting procedure and the residual asymmetry corrections are added in quadrature and scaled by the dilution factor, $F_{B_s^0}^{\text{osc}}$. The effect of the uncertainty on the dilution factor is then added in quadrature, giving a total systematic uncertainty of 0.17%.

The resulting time-integrated flavor-specific semileptonic charge asymmetry is found to be

$$a_{\text{sl}}^s = [-1.08 \pm 0.72 (\text{stat}) \pm 0.17 (\text{syst})] \% \quad (7)$$

superseding the previous measurement of a_{sl}^s by the D0 Collaboration [4, 16] and in agreement with the SM prediction. This result can be combined with the two A_{sl}^b measurements that depend on the impact parameter of the muons (IP) [3] and the average of a_{sl}^d measurements from the B factories, $a_{\text{sl}}^d = (-0.05 \pm 0.56)\%$ [14],

(Fig. 3). As a result of this combination we obtain $a_{\text{sl}}^s = (-1.40 \pm 0.57)\%$ and $a_{\text{sl}}^d = (-0.22 \pm 0.32)\%$ with a correlation of -0.54 , which is a significant improvement on the precision of the measurement of a_{sl}^d and a_{sl}^s obtained in Ref. [3]. These results have a probability of agreement with the SM of 0.30×10^{-2} , which corresponds to a 3.0 standard deviations from the SM prediction.

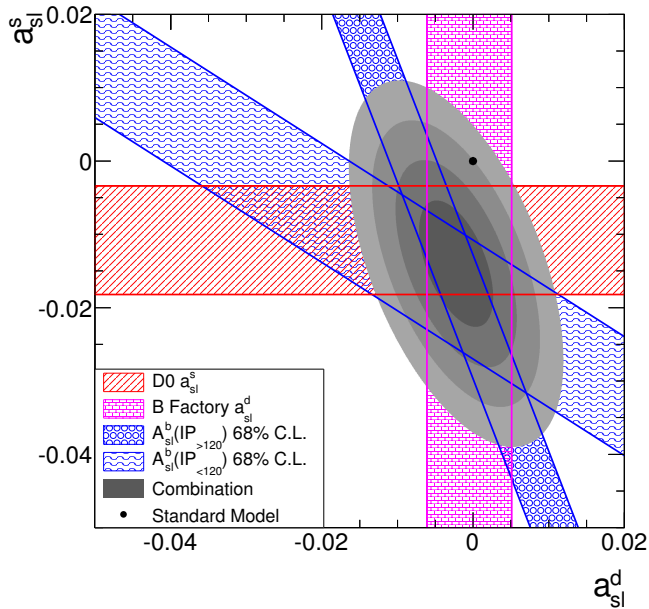


FIG. 3: (color online) A combination of this result with two measurements of A_{sl}^b with different muon impact parameter selections made using like-sign dimuons [3] and the average of a_{sl}^d measurements from B factories [14]. The error bands represent the ± 1 standard deviation uncertainties on each individual measurement. The ellipses represent the 1, 2, 3, and 4 standard deviation two-dimensional C.L. regions, respectively, in the a_{sl}^s and a_{sl}^d plane.

In summary, we present the most precise measurement of the time-integrated flavor-specific semileptonic charge asymmetry. When this result is combined with the like-sign dimuons results [3] and the world average value of a_{sl}^d we extract a value of $a_{\text{sl}}^s = (-1.40 \pm 0.57)\%$ with is 2.5 standard deviations from the SM prediction.

We thank the staffs at Fermilab and collaborating institutions, and acknowledge support from the DOE and

NSF (USA); CEA and CNRS/IN2P3 (France); MON, NRC KI and RFBR (Russia); CNPq, FAPERJ, FAPESP and FUNDUNESP (Brazil); DAE and DST (India); Colciencias (Colombia); CONACyT (Mexico); NRF (Korea); FOM (The Netherlands); STFC and the Royal Society (United Kingdom); MSMT and GACR (Czech Republic); BMBF and DFG (Germany); SFI (Ireland); The Swedish Research Council (Sweden); and CAS and CNSF (China).

- [1] A. Lenz and U. Nierste, arXiv:1102.4274; A. Lenz and U. Nierste, *J. High Energy Phys.* **06**, 072 (2007).
- [2] V. M. Abazov *et al.* (D0 Collaboration), *Phys. Rev. D* **82**, 032001 (2010); V. M. Abazov *et al.* (D0 Collaboration), *Phys. Rev. Lett.* **105**, 081801 (2010).
- [3] V. M. Abazov *et al.* (D0 Collaboration), *Phys. Rev. D* **84**, 052007 (2011).
- [4] V. M. Abazov *et al.* (D0 Collaboration), *Phys. Rev. D* **82**, 012003 (2010).
- [5] V.M. Abazov *et al.* (D0 Collaboration), *Nucl. Instrum. Methods Phys. Res. A* **565**, 463 (2006).
- [6] R. Angstadt *et al.* (D0 Collaboration), *Nucl. Instrum. Meth. A* **622**, 278 (2010).
- [7] $\eta = -\ln[\tan(\theta/2)]$ is the pseudorapidity and θ is the polar angle between the track momentum and the proton beam direction. ϕ is the azimuthal angle of the track.
- [8] V.M. Abazov *et al.* (D0 Collaboration), *Nucl. Instrum. Meth. A* **552**, 372 (2005).
- [9] J. Abdallah *et al.* (DELPHI Collaboration), *Eur. Phys. J. C* **32**, 185 (2004).
- [10] V. M. Abazov *et al.* (D0 Collaboration), *Phys. Rev. Lett.* **97**, 021802 (2006).
- [11] G. Borisov, *Nucl. Instrum. Methods Phys. Res. A* **417**, 384 (1998).
- [12] T. Sjöstrand, S. Mrenna and P. Z. Skands, *J. High Energy Phys.* **05**, 026 (2006).
- [13] D.G. Lange, *Nucl. Instrum. Methods in Phys. Res. A* **462**, 152 (2001); for details see <http://www.slac.stanford.edu/~lange/EvtGen>.
- [14] D. Asner *et al.*, Heavy Flavor Averaging Group (HFAG), arXiv:1010.1589; making use of the 2012 update: http://www.slac.stanford.edu/xorg/hfag/osc/PDG_2012/
- [15] R. Aaij *et al.*, (LHCb Collaboration), arXiv:1202.4717; R. Aaij *et al.*, (LHCb Collaboration), *Phys. Rev. Lett.* **108**, 101803 (2012).
- [16] The analysis presented in this Letter has the same statistical uncertainty as the analysis presented in Ref. [4] when performed on the same data sample.